# Reconfigurable Infrared Ellipse-Shape Metamaterial

Zihao Liang, Zhicheng Lin, Pengyu Liu, Zhi Zhang, Xiao Zhang, Zefeng Xu, Xiaocan Xu, Zhaokang Liang, Zheng Song, Chao Tang, Jie Lin, Haolin Deng, Zhenwei Dai, Yao Wen, Ruijia Xu, Dongyuan Yao, and Yu-Sheng Lin*
*State Key Laboratory of Optoelectronic Materials and Technologies,*
*School of Electronics and Information Technology, Sun Yat-Sen University,*
Guangzhou, China
linyoush@mail.sysu.edu.cn

***Abstract*—The designs of cross ellipse-shape metamaterial (ESM) in infrared (IR) wavelength range are presented. They are composed of a tailored gold (Au) layer on silicon (Si) substrate. The characterizations of proposed devices can be manipulated their electromagnetic responses between single-band and dual-band resonances by changing different ratio of macro-axis and minor-axis of ESM. The electromagnetic behavior of dual-band resonance exhibits the resonance with broad bandwidth or narrow bandwidth, while the corresponding free spectral range (FSR) could be controlled from 0.154 μm to 0.607 μm depending on the design of symmetrical or asymmetrical ESM. According to these optical characteristics of cross ESM, we can design ESM-like nanostructures to realize IR filter, polarization switch, band switch, and high-efficiency sensor applications.**

***Keywords*—metamaterial, infrared filter, resonator**

## I. Introduction

Metamaterials have unique electromagnetic characteristics that are unable to be found in natural materials and have great research values [1-3], such as negative refraction index and invisible cloaking [4-6]. In view of these merits of metamaterials, there have been reported many literatures to demonstrate metamaterials used in widespread applications, such as sensor, switch, filter, etc. By properly tailoring the geometrical dimension of metamaterial, the electromagnetic behaviors can be manipulated, e.g. amplitude, wavelength, phase, and polarization [2-7].

In this study, we propose a series of designs of cross ellipse-shape metamaterial (ESM) with different ratio of the minor-axis and the macro-axis of each design in infrared (IR) spectrum range. The designs of cross ESM are composed of a textured Au layer on Si substrate, which shows switch function of single-band to dual-band resonances, and tunable free spectral range (FSR). These characteristics can be contributed to the arrangement of minor-axis and the macro-axis of ESM. The proposed ESM are simple structures, easy to manufacture, and low cost. Such strategy provides the great potential uses for next generation IR opto-electronic devices.

## II. Materials and Methods

The composition of proposed device is a tailored 200-nm-thick Au layer with cross ellipse-shape on Si substrate. We define the ratio of minor-axis ($b$) and the macro-axis ($a$) of ESM as $r = b/a$. For the discussion of the influence of $r$ value, $a$ value is kept as constant while $b$ value is variable. The period of cross ESM is kept as constant as $P_x = P_y = 3$ μm. The schematic drawing of proposed device is indicated in the inserted image of Fig. 1(a). When changing the ratio ($r = b_1/a_1 = b_2/a_2$), two ESMs are varied simultaneously. It means the electromagnetic behaviors are identical at TE and TM modes. The relationships of resonance and $r$ value of cross ESM are summarized in Fig. 1(a). Fig. 1(b) shows the corresponding E-field and H-filed distributions of $r$ = 0.2, 0.5, 0.8, and 1.0, respectively. It can be seen that E-field and H-field energies are focused on two sides of the lateral ESM.

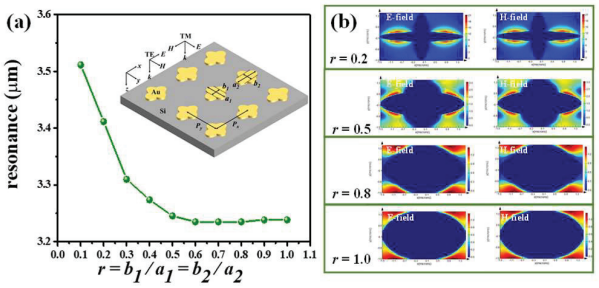


Fig. 1. (a) The relationship of resonance and $r$ value. Inserted schematic drawing is the proposed cross ESM device. (b) The E-field and H-filed distributions of cross ESM with $r$ = 0.2, 0.5, 0.8, and 1.0, respectively.

## III. Results and Discussions

To figure out the influence of changing $r_2$ with different $r_1$ value, the $r_1$ value is kept as constant as 0.1 and $r_2$ is varied from 0.1 to 1.0 as shown in Fig. 2. Fig. 2(a) and (b) show the transmission spectra of cross ESM with different $r_2$. The electromagnetic response is single-band and polarization-independent with a resonance dip ($\omega_0$) at 3.104 μm for $r_2$ varied from 1.0 to 0.9 at TE and TM modes. When $r_2$ is 0.8, the resonance becomes polarization-dependent that has two resonances ($\omega_1$ = 3.005 μm and $\omega_2$ = 3.238 μm) at TE mode, and ($\omega_1$ = 3.011 μm and $\omega_2$ = 3.299 μm) at TM mode. At TE mode, the electromagnetic response is nearly identical for $r_2$ is 0.7 and 0.6. When $r_2$ is varied from 0.5 to 0.2, resonance dip ($\omega_0$) is vanished and there are two resonant peaks ($\omega_1$ and $\omega_2$) varied from 3.002 μm to 3.029 μm and from 3.193 μm to 3.373 μm for $\omega_1$ and $\omega_2$, respectively. The corresponding tuning ranges are 27 nm and 180 nm. At TM mode, there are two resonant peaks for $r_2$ varying from 0.8 to 0.2. The tuning range of $\omega_1$ is 30 nm from 3.011 μm to 3.041 μm and that of $\omega_2$ is 349 nm from 3.299 μm to 3.648 μm. The tuning ranges of FRS are 135 nm from 0.368 to 0.233 μm and from 0.288 to 0.607 μm for TE and TM modes.

Fig. 3(a) shows the relationship of resonance and $r_2$ of cross ESM kept $r_1$ as constant as 0.1. The electromagnetic response of cross ESM with different $r_2$ exhibits hysteresis behavior at TE and TM modes. To better understand the electromagnetic behaviors of varying $r_2$ under the different $r_1$ value, the relationships of resonance peak ($\omega_2$) and $r_2$ of cross ESM under the conditions of $r_1$ = 0.3 and $r_1$ = 0.5 are shown in Fig. 3(b) and (c), respectively. The results exhibit the hysteresis behavior at TE and TM modes, which are identical to those in Fig. 3(a). The TM response is overall blue-shifted by increasing $r_1$ value and then saturated and kept stable at 3.23 μm. While the trend of TE response is approximately unchanged by increasing $r_1$ value. This can be explained by keeping $a_2$ as constant and changing $b_2$ to define different $r_2$

978-1-7281-4503-7/19/$31.00 ©2019 IEEE

along y-direction of ESM. The electromagnetic characteristics of cross ESM at TE mode mainly depends on the horizontal ESM while those of cross ESM at TM mode mainly depends on the vertical ESM. Fig. 3(d) shows the E-field and H-filed distributions of $r_2$ = 0.2, 0.5, 0.8, and 1.0, respectively under the condition of $r_1$ = 0.1. The E-field energy is focused on top and bottom sides of horizontal ESM (along x-direction) while the H-field energy is focused on top and bottom sides of vertical ESM (along y-direction). It is clearly explained the characteristics of electromagnetic response at TE mode mainly depends on the horizontal ESM while that at TM mode mainly depends on the vertical ESM.

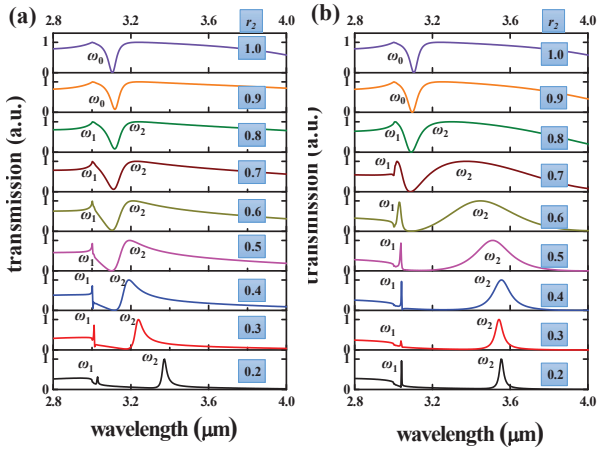


Fig. 2. Transmission spectra of cross ESM with different $r_2$ value at (a) TE mode and (b) TM mode. The $r_1$ is kept as constant as 0.1.

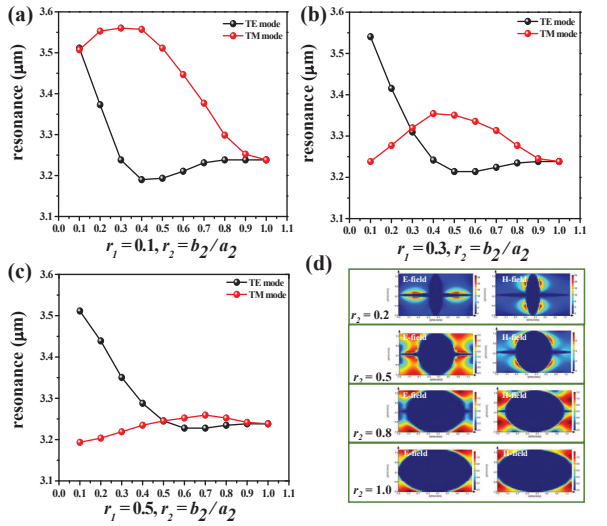


Fig. 3. The relationships of resonance and $r_2$ value for cross ESM under the conditions of (a) $r_1$ = 0.1, (b) $r_1$ = 0.3, and (c) $r_1$ = 0.5. (d) The E-field and H-filed distributions of cross ESM with $r_2$ = 0.2, 0.5, 0.8, and 1.0, respectively under the condition of $r_1$ = 0.1.

Fig. 4(a) shows the schematic drawing of dual-layer ESM. This dual-layer ESM is designed with a gap between top and bottom ESM ($h$). The electromagnetic responses of dual-layer ESM can be tuned by changing $h$ value using MEMS technique. The $r_1$ and $r_2$ values are 0.5 μm. The corresponding E-field and H-field distributions are shown in Fig. 4(b) and (c), respectively. The electromagnetic energy distributions are similar to the those of single-layer ESM concentrated on four corners of ESM. Fig. 4(d) shows the transmission spectra of dual-layer ESM with different $h$ value at TE mode. The bandwidth of resonance ($\omega_0$) becomes broader at 3.050 μm.

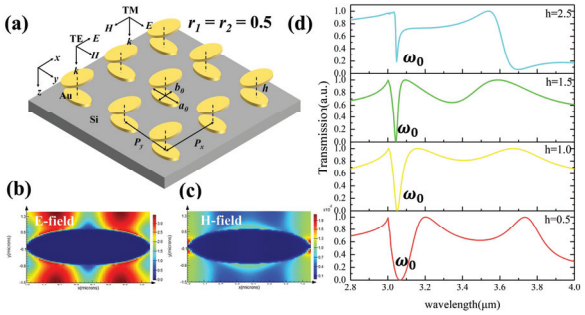


Fig. 4. (a) Schematic drawing of dual-layer ESM with $r_1$ = $r_2$ = 0.5. The corresponding E-field and H-field contributions are shown in (b) and (c), respectively. (d) The transmission spectra of dual-layer ESM with different $h$ value at TE mode.

## IV. Conclusion

In conclusion, we present the reconfigurable IR ESMs and study the influences of electromagnetic characteristics by changing the minor-axis and the macro-axis of ESM. The electromagnetic response can be manipulated between single-band and dual-band resonances by changing different ratio of macro-axis and minor-axis of ESM. By varying $r$ value, the electromagnetic behavior of dual-band resonance can be tuned from broad bandwidth to narrow bandwidth, while the corresponding FSR could be controlled from 154 nm to 607 nm depending on the design of symmetrical or asymmetrical ESM. These characteristics can be used to realize filter, optical switch, and environment sensor in IR wavelength range.

## Acknowledgment

The authors acknowledge the financial support from research grants of 100 Talents Program of Sun Yat-Sen University (grant number 76120-18841202) and the State Key Laboratory of Optoelectronic Materials and Technologies of Sun Yat-Sen University for the use of experimental equipment.

## References

[1] C. M. Soukoulis, and M. Wegener, "Past achievements and future challenges in the development of three-dimensional photonic metamaterials," *Nat. Photonics*, vol. 5, pp. 523-530, 2011.

[2] Y. S. Lin and W. Chen, "A large-area, wide-incident-angle, and polarization-independent plasmonic color filter for glucose sensing," *Opt. Mater.*, vol. 75, pp.739-743, 2018.

[3] J. Valentine, S. Zhang, T. Zentgraf, E. Ulin-Avila, D. A. Genov, G. Bartal, and X. Zhang, "Three-dimensional optical metamaterial with a negative refractive index," *Nature*, vol. 455, pp. 376-379, 2008.

[4] Y. S. Lin and W. Chen, "Perfect meta-absorber by using pod-like nanostructures with ultra-broadband, omnidirectional, and polarization-independent characteristics," *Sci. Rep.*, vol. 8, pp. 7150, 2018.

[5] B. Gholipour, J. Zhang, K. F. MacDonald, D. W. Hewak, and N. I. Zheludev, "An All-Optical, Non-volatile, Bidirectional, Phase-Change Meta-Switch," *Adv. Mater.*, vol. 25, pp. 3050-3054, 2013.

[6] R. Xu, J. Luo, J. Sha, J. Zhong, Z. Xu, Y. Tong, and Y. S. Lin, "Stretchable IR metamaterial with ultra-narrowband perfect absorption," *Appl. Phys. Lett.*, vol. 113, pp. 101907, 2018.

[7] Y. S. Lin, "Complementary Infrared Metamaterials for Volatile Organic Solutions Sensing," *Mater. Lett.*, vol.195, pp.55-57, 2017